

## Original Article

# Quantification methods comparison in brain <sup>18</sup>F-FDOPA PET

Julieta E Arena<sup>1\*</sup>, Leandro Urrutia<sup>2\*</sup>, German Falasco<sup>2</sup>, Magdalena Ponce de Leon<sup>2</sup>, Silvia Vazquez<sup>2</sup>

<sup>1</sup>Movement Disorders Section, Department of Neurology, Fleni. Montañeses 2325, C1428AQK, Ciudad Autónoma de Buenos Aires, Argentina; <sup>2</sup>Molecular Imaging Department, Fleni. Ruta 9, Km 52.5, B1625XAF Escobar, Buenos Aires, Argentina. \*Equal contributors.

Received September 27, 2019; Accepted December 11, 2019; Epub December 15, 2019; Published December 30, 2019

**Abstract:** <sup>18</sup>F-FDOPA PET is one of the most widely used molecular imaging techniques to assess presynaptic dopaminergic activity. A variety of analytical methods have been developed to quantify <sup>18</sup>F-FDOPA PET images and in most, the striatal-to-occipital ratio (SOR) is used as a quantitative parameter. A manual strategy is typically used for quantification purposes, which can have some caveats, being time-consuming and having some inter-rater variability. In the present study we aimed to test whether automated quantification methods can provide an efficient alternative to manual quantification to overcome its limitations and compare each method's capacity to discriminate between normal and abnormal subjects. <sup>18</sup>F-FDOPA PET images of 60 subjects were analyzed and quantified with one manual and two automated methods. SUVRs were obtained for caudate and putamen nucleus in both cases. We were able to reach the same level of discrimination with manual and automated strategies, and a threshold for normal/abnormal discrimination could be obtained. We believe automated strategies for VOI quantification can help molecular imaging physicians in the process of interpretation of studies, making the process faster, yet reliable and objective.

**Keywords:** <sup>18</sup>F-FDOPA PET, quantification, parkinsonism, PET quantification methods

### Introduction

Parkinson's disease (PD) is the second most common neurodegenerative disease. Its clinical symptoms include several motor and non-motor symptoms, including tremor, rigidity and bradykinesia. PD is nowadays understood as a multi-system disorder, but its most important neurotransmitter alteration is the dopamine (DA) loss in the striatum.

There are several ways to assess dopaminergic activity *in-vivo* through molecular imaging. The measurement of dopaminergic activity can give us an indirect insight of the dopaminergic structures integrity.

<sup>18</sup>F-FDOPA PET is one of the most widely used molecular imaging methods to assess presynaptic dopaminergic activity, measuring the activity of the L-aromatic amino acid decarboxylase (AADC), which is one of the most important enzymes in DA synthesis, responsible of

turning levodopa into DA. A manual strategy is typically used for quantification purposes.

<sup>18</sup>F-FDOPA uptake has been proved to have a good correlation with dopaminergic cell count and is relatively preserved in early disease, probably aided by a compensatory upregulation of AADC in early stages [1].

A variety of analytical methods have been developed to quantify <sup>18</sup>F-FDOPA PET images [2-4], and in most, the striatal-to-occipital ratio (SOR) is used as a quantitative parameter. This has provided useful and enough information with target-to-background calculations, as it is done with a tissue reference approach.

A manual strategy is typically used for quantification purposes. The SOR is generally calculated using volumes of interest (VOIs) manually drawn in the striatum and the occipital area; either over the PET image guiding the localization of the VOIs by the activity; or the coregis-

tered image of magnetic resonance (MRI) for better anatomical precision. Although this is a widely used technique, manual VOI positioning can be time-consuming and can have inter-rater variability, being such an operator-dependent procedure.

In the present study we aimed to test whether automated quantification methods can provide an efficient alternative to manual quantification to overcome its limitations.

We tested two methods in which normalized images were generated and previously defined ROIs (either manually over a template or atlas-derived, in each case) were automatically applied over the PET image for quantification.

We then aimed to compare each method's capacity to discriminate normal or abnormal images, as determined by qualitative analysis by molecular imaging specialists.

### Materials and methods

Imaging studies of 60 subjects with a clinical diagnosis of parkinsonism, to whom a  $^{18}\text{F}$ -FDOPA PET was ordered for clinical purposes by a movement disorders specialist, were tested. The study was approved by the research ethics committee of our institution. The sample consisted of 20 women and 40 men; mean [SD] age at the moment of the scan, 59.7 [12.8] years; range 35.7-82.3 years.

23 had a suspected diagnosis of Parkinson's disease, 9 were studied for tremor, the rest had other parkinsonisms suspected including atypical parkinsonisms, pharmacologic parkinsonism, and psychogenic disorders.

Antiparkinsonian medications (if taken) were stopped overnight, and subjects were given 200 mg of carbidopa 1 hour before the  $^{18}\text{F}$ -FDOPA administration. PET acquisition was performed (Ge690 PET scanner) 50 min after injection of 370 MBq of  $^{18}\text{F}$ -FDOPA. PET images were reconstructed using the OSEM algorithm (2 iterations, 24 subsets).

MRI was available for 12 subjects using a T1-3D sequence on a GE Discovery MR750.

A qualitative analysis of the images was performed by two specialists. Images were quali-

fied as having either normal uptake (NU) or decreased uptake (DU).

The image was considered to have a DU when it had either a global decrease, a bilateral yet asymmetric decrease, or a unilateral asymmetric decrease in the uptake.

As a first approach, a strategy of manual quantification was implemented. After that, two alternative strategies (semi-automated and automated) were proposed, based on the spatial normalization of brain images to a standardized space (details of each method are described below).

Quantification VOIs were defined over the PET image according to different strategies, one on manually pre-defined regions in a template of  $^{18}\text{F}$ -FDOPA, and another one based on atlas. Finally, the validity of the methods was tested against the manual strategy and their ability in the discrimination of groups based on their agreement with the qualitative visual analysis.

### Manual strategy (MS)

Keeping in mind that  $^{18}\text{F}$ -FDOPA PET has a good *signal-to-noise* ratio, it is possible to determine the VOIs directly over the PET image, without the anatomic reference of the patient's MRI, as it has been shown for RAC PET scans [5].

VOIs were previously defined in an  $^{18}\text{F}$ -FDOPA template [6]. The total volume of the human adult striatum is 20 cm<sup>3</sup> approximately [7], but not all of it is sampled for the analysis. According to Mai and colleagues, an estimate of the area at the midpoint of the striatum is approximately 180 mm<sup>2</sup>, or 360 mm<sup>2</sup> bilaterally [8]. For our study, a combination of circles and ellipses was used to delineate caudate and putamen over transaxial images [9]. The area of all VOIs bilaterally in each slice was of 363 mm<sup>2</sup>, and was applied in 6 consecutive slices over the template (each slice of 3.27 mm) accounting for a total thickness of 19.62 mm in which the caudate and putamen were best visualized. For the occipital reference region the VOIs were applied in only 4 slices (**Figure 1**).

Subsequently, the previously delineated VOIs were placed manually over the PET images by an experienced *physician*, choosing the slices with the highest activity [7] to define the cau-

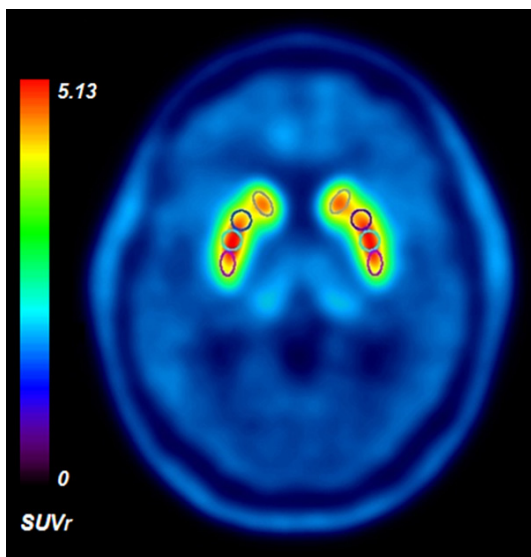


**Figure 1.** Representative image of  $^{18}\text{F}$ -FDOPA PET image with manually placed striatal ROIs for quantification.

date and putamen; and divide the latter in its anterior, medium and posterior parts (**Figure 1**).

#### *Semi-automated and automated strategies*

$^{18}\text{F}$ -FDOPA images of each subject were transformed into a standardized space using the SPM software (Wellcome Trust Centre for Neuroimaging). A  $^{18}\text{F}$ -FDOPA template [6] was used as reference. Spatial processing included the designation of a common image origin, co-registration and standardization to the template.

In the semi-automated strategy the VOIs previously defined on the FDOPA template (as described for the manual strategy) were applied automatically over the normalized images, and mean VOI intensities were calculated for quantification (since the VOIs derived from the previous method, we have designated this one Semi-Automated Strategy-SAS).

In the automated strategy (AS), the same normalized images were used, but the VOIs applied corresponded to caudate and putamen designation from the Desikan-Killiany-Tourville atlas (DKT) [10]. DKT VOIs were adjusted with a spatial restriction on the number of slices, using the same number and position on the coronal plane as for  $^{18}\text{F}$ -FDOPA template VOI designation.

While the AS used DKT-derived VOIs in order to make a better anatomical definition of the basal ganglia, it did not use each subjects' MRI. Instead, VOIs were placed automatically over the normalized PET image.

In order to prove that this was comparable with defining the VOIs over each subject's MRI, 12 subjects which had an MRI available underwent another quantification method also using the DKT-derived VOIs, this time defined in each subject's MRI space (FreeSurfer process, FS\_MRI).

#### *Methodologies comparison*

Agreement between different methodologies was evaluated through Bland-Altman plots. These graphs were generated for the comparison of both, SAS (**Figure 2**) and AS (**Figure 3**), with respect to the manual strategy, which was considered as the reference quantitative method.

Quantitative data for each comparison (mean values of the differences, standard deviation and limits of agreement for 95% of the sample) is summarized in **Table 1**. The same variables were calculated for the NU and DU groups, also subdivided into caudate and putamen. The overall results were also expressed as caudate and putamen SUVR without group distinction (NU vs. DU).

#### *Group classification performance*

Boxplot graphics (**Figure 4**) were generated to evaluate overall distribution on the quantitative striatum value and analyze mean differences between NU and DU groups for each methodology.

Performance in NU and DU group classification was evaluated with a ROC (Receiver Operating Characteristic) curve analysis using whole striatum quantification for each methodology (**Figure 5**). Assuming the qualitative clinical designation as a criterion for the correct group classification, it was possible to evaluate the performance of each methodology, based on the AUC (Area Under Curve) indicator, in terms of the level of sensitivity and specificity for variable threshold settings. Said analysis additionally indicated the optimum threshold in the quantitative value, based on obtaining the best

## Quantification in $^{18}\text{F}$ -FDOPA PET

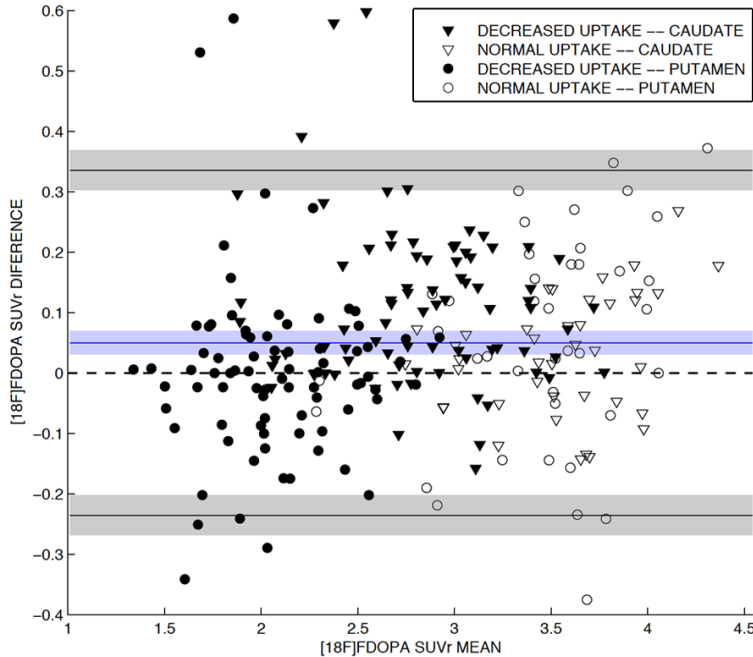


**Figure 2.** Bland Altman plot Manual vs. Semiautomatic strategies.  $^{18}\text{F}$ -FDOPA SUVR for bilateral caudate and putamen. Blue line: mean difference. Black lines: superior and inferior limits of agreements for 95% of the data.

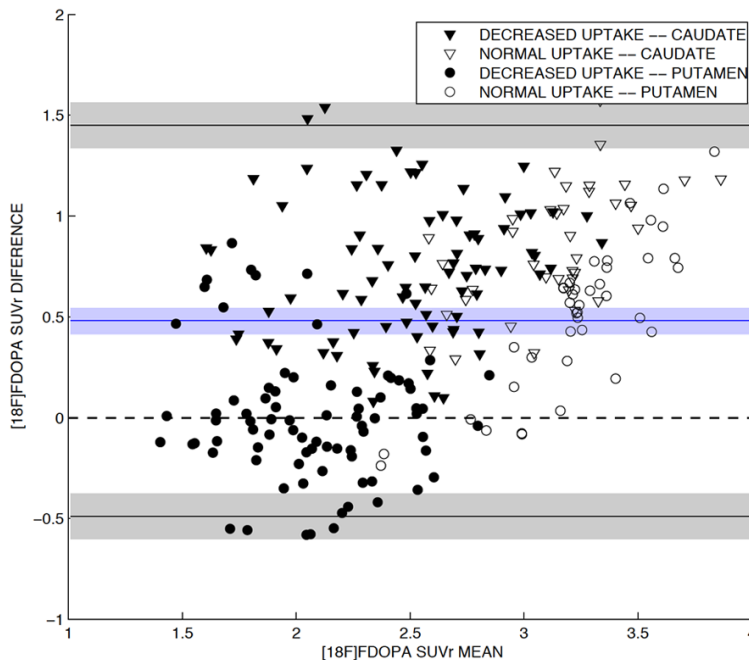


**Figure 3.** Bland Altman plot Manual vs. Automatic strategies.  $^{18}\text{F}$ -FDOPA SUVR for bilateral caudate and putamen. Blue line: mean difference. Black lines: superior and inferior limits of agreements for 95% of the data.

sensitivity and specificity simultaneously in subject discrimination.

+ Putamen) by the three methods, discriminating subjects with normal and decreased uptake

## Results

### Qualitative evaluations

As a first step we have delineated a Bland Altman plot with the SUVR values for Caudate and Putamen of each side for all subjects, as determined by the MS and SAS (Figure 2). We could observe an acceptable dispersion of the SUVR values that remained stable along the mean value axis. The mean difference indicates a slightly trend on MS to result in higher values than SAS (0.050). As verified in Table 1, this trend could be attributed to caudate structure (0.083), principally in the DU group (0.109).

The same plot was performed for the MS vs. AS comparison (Figure 3) and showed a similar pattern of dispersion but with significantly higher differences (0.481). Again, differences are principally due to caudate quantification (Table 1, 0.793), showing higher values with the MS, but in this case in both the NU and DU groups.

In this comparison, higher values for the putamen could also be observed (0.168), obtaining higher values with the MS, specifically for the NU group (0.507).

Taking the striatum as a whole, subjects with NU showed higher SUVR values with the MS than with the AS (0.703).

To further evaluate the reliability of the automated methods in  $^{18}\text{F}$ -FDOPA quantification we compared the uptake in the striatum as a whole (Caudate

**Table 1.** Statistical resume for Bland Altman plots

	MANUAL VS. SEMIAUTOMATIC				MANUAL VS. AUTOMATIC			
	Mean	STD	Sup_95	Inf_95	Mean	STD	Sup_95	Inf_95
DU								
CAUDATE + PUTAMEN	0.054	0.147	0.342	-0.234	0.369	0.495	1.339	-0.601
CAUDATE	0.109	0.131	0.364	-0.147	0.739	0.335	1.396	0.083
PUTAMEN	-0.001	0.143	0.278	-0.281	-0.001	0.321	0.628	-0.630
NU								
CAUDATE + PUTAMEN	0.043	0.144	0.325	-0.238	0.703	0.414	1.514	-0.108
CAUDATE	0.031	0.099	0.225	-0.162	0.899	0.366	1.616	0.183
PUTAMEN	0.055	0.178	0.404	-0.294	0.507	0.366	1.225	-0.211
NU + DU								
CAUDATE + PUTAMEN	0.050	0.146	0.336	-0.235	0.481	0.494	1.449	-0.488
CAUDATE	0.083	0.126	0.330	-0.164	0.793	0.352	1.483	0.103
PUTAMEN	0.018	0.157	0.325	-0.290	0.168	0.413	0.977	-0.641

DU: Decreased Uptake; NU: Normal Uptake; Mean: mean of the differences; STD: Standard deviation of the differences; Sup\_95 and Inf\_95: superior and inferior limits of agreements where 95% of the differences will lie.

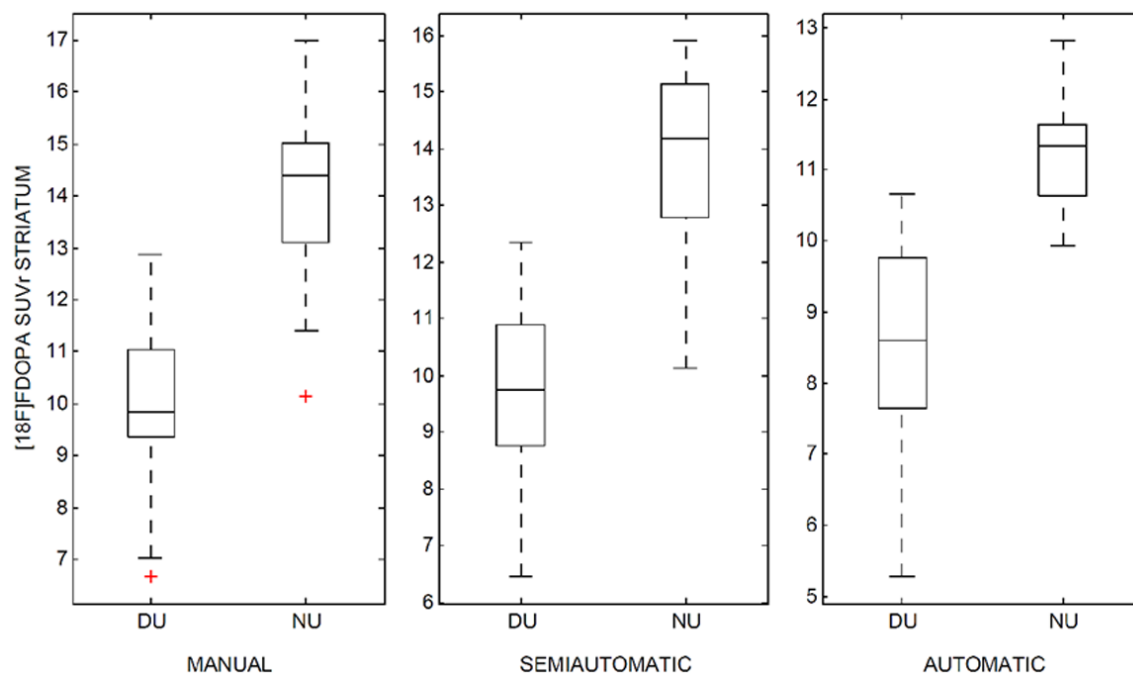


**Figure 4.** <sup>18</sup>F-FDOPA Striatum SUVR value boxplot distribution for each method. NU: Normal Uptake. DU: Decrease Uptake.

and were able to see how values compare in all of them. Using boxplots, the MS and the SAS showed very similar results. The AS showed a reduced dispersion of the data in the NU group (Figure 4).

ROC curves using the SUVR values for the whole striatum were used to evaluate the ability of each method to distinguish between sub-

jects with normal and decreased uptake. Resulted curves shown they all succeeded to do so (Figure 5). The AUC was of 0.965 for the MS, 0.976 for the SAS, and 0.985 for the AS.

A threshold for subject discrimination (NU vs. DU) was obtained for each methodology, throwing similar values for MS and SAS (3.08 and 3.05), and a lower one for AS (2.57).



## Quantification in $^{18}\text{F}$ -FDOPA PET

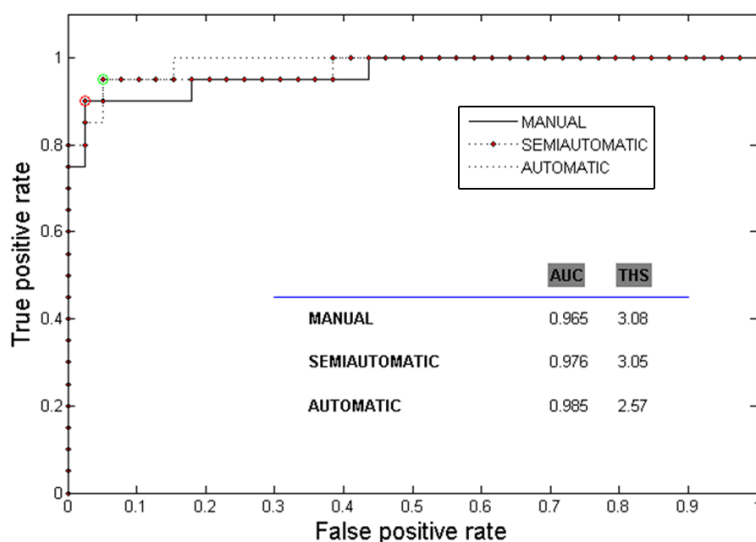


**Figure 5.** ROC curves (Manual, Semiautomatic, Automatic) of  $^{18}\text{F}$ -FDOPA Striatum SUVr values for group discriminant between normal and decrease uptake. AUC: Area under the curve, TSH: Optimal threshold for discrimination. True/False positive rates for optimal threshold (green: Automatic; red: Manual and Semiautomatic).

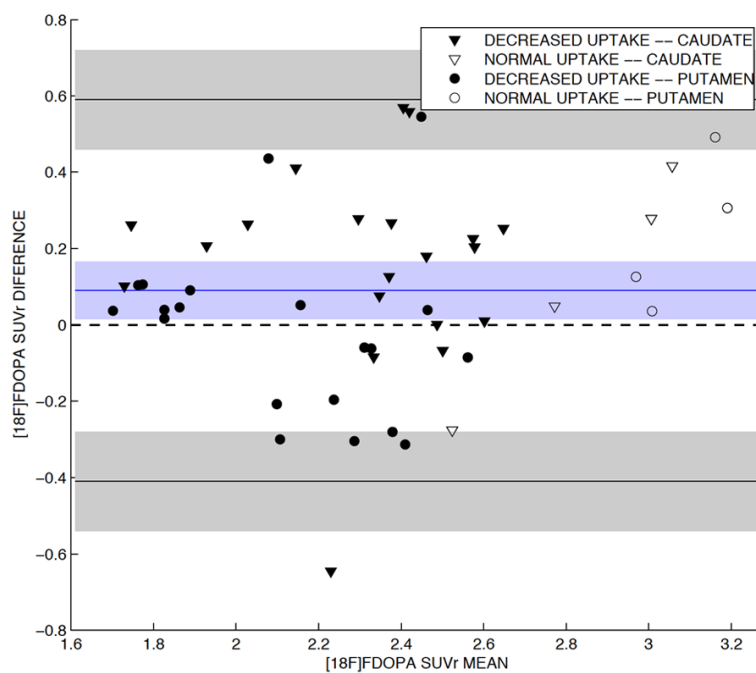


**Figure 6.** Bland Altman plot FS\_MRI vs. Automatic strategy.  $^{18}\text{F}$ -FDOPA SUVr for bilateral caudate and putamen. Blue line: mean difference. Black lines: superior and inferior limits of agreements for 95% of the data.

In the 12 subjects in whom an MRI was available (FS\_MRI), VOI definition over the anatomical image was tested against VOI definition in the AS. An acceptable dispersion of the SUVr values was observed (**Figure 6**), succeeding to

prove the accuracy of VOI definition without MRI guidance. Quantification values are compared in **Table 2**.

### Discussion

In the present study we successfully tested two automated methods for  $^{18}\text{F}$ -FDOPA PET quantification in patients with suspected parkinsonism.

While the first automated strategy (SAS) still uses the previously manually drawn VOI over the template and automatically placed on normalized images (to overcome the bias introduced by manual selection of areas with higher activity); the second one still uses the image in the normalized space, but using a version of a VOI defined in the same space over an MRI T1 template to make it more anatomically accurate.

Regarding the degree of concordance of the methodologies studied, we could observe that similar quantitative results are obtained with the manual and semi-automated strategies, indicating that the spatial normalization process involved in SAS but not in MS, has only a slight incidence in the quantified values. Slightly higher values were found with the MS, more specifically in the caudate VOI, and we hypothesize that this could be due to the fact that manually placing the VOI over the PET image probably better 'chooses' the sites of higher uptake.

Comparing the MS with the AS also showed higher values for the caudate uptake for the former. The greatest difference observed with the SA method can be then attributed to the use of VOIs that differ from those used in MS and SAS, since their origin is based on anatomical delimitations estab-

**Table 2.** Statistical resume for Bland Altman plots

	FS_MRI VS. AUTOMATIC			
	Mean	STD	Sup_95	Inf_95
DU				
CAUDATE + PUTAMEN	0.073	0.256	0.574	-0.429
CAUDATE	0.160	0.259	0.667	-0.347
PUTAMEN	-0.015	0.227	0.430	-0.460
NU				
CAUDATE + PUTAMEN	0.178	0.247	0.663	-0.306
CAUDATE	0.117	0.302	0.710	-0.476
PUTAMEN	0.240	0.202	0.636	-0.156
NU + DU				
CAUDATE + PUTAMEN	0.090	0.255	0.590	-0.410
CAUDATE	0.153	0.260	0.662	-0.357
PUTAMEN	0.028	0.239	0.497	-0.441

DU: Decreased Uptake; NU: Normal Uptake; Mean: mean of the differences; STD: Standard deviation of the differences; Sup\_95 and Inf\_95: superior and inferior limits of agreements where 95% of the differences will lie.

lished on MRI images. In this case, VOIs cover larger regions than the VOIs defined on the F-DOPA template, which focus on the region with higher uptake. This is reflected in the increased limits of agreement when comparing MS vs. AS in the Bland Altman chart (**Figure 3**).

In all the previously mentioned comparisons, the results described expected differences in the absolute values quantified, and how different methods resemble or differ in their findings.

The capacity of each method in the identification of pathological subjects was also evaluated in this study. In this respect, a good segregation between subjects with normal and decreased uptake could be obtained when quantifying caudate and putamen separately (this can be observed along the mean value axis for both of the proposed methodologies in **Figures 2 and 3**). This was also verified for whole striatum quantification (**Figure 4**).

ROC curves support these results and show that we were able to find a good agreement of each method with the qualitative designation made by two trained and experienced physicians. These results are comparable to previous studies in which the MRI of each subject was used for VOI delineation [11].

We were also able to determine a threshold between normal and abnormal studies.

In essence, based on spatial normalization and testing two different ways of VOI delineation, we believe we were able to overcome the time-consuming and operator-dependent process of manual VOI delineation, reaching the same level of discrimination, and also avoiding the need to use each subjects' MRI images for the VOI delineation.

We believe automated strategies for VOI quantification can help molecular imaging physicians in the process of interpretation of studies, making the process faster, yet reliable and objective.

#### Disclosure of conflict of interest

None.

**Address correspondence to:** Julieta E Arena, Movement Disorders Section, Department of Neurology, Fleni. Montañeses 2325, C1428-AQK, Ciudad Autónoma de Buenos Aires, Argentina. Tel: +541157773200; E-mail: jarena@fleni.org.ar

#### References

- [1] Lee CS, Samii A, Sossi V, Ruth TJ, Schulzer M, Holden JE, Wudel J, Pal PK, de la Fuente-Fernandez R, Calne DB and Stoessl AJ. In vivo positron emission tomographic evidence for compensatory changes in presynaptic dopaminergic nerve terminals in Parkinson's disease. *Ann Neurol* 2000; 47: 493-503.
- [2] Takikawa S, Dhawan V, Chaly T, Robeson W, Dahl R, Zanzi I, Mandel F, Spetsieris P and Eidelberg D. Input functions for 6-[fluorine-18] fluorodopa quantitation in parkinsonism: comparative studies and clinical correlations. *J Nucl Med* 1994; 35: 955-963.
- [3] Dhawan V, Ma Y, Pillai V, Spetsieris P, Chaly T, Belakhlef A, Margouleff C and Eidelberg D. Comparative analysis of striatal FDOPA uptake in Parkinson's disease: ratio method versus graphical approach. *J Nucl Med* 2002; 43: 1324-1330.
- [4] Jokinen P, Helenius H, Rauhala E, Brück A, Eskola O and Rinne JO. Simple ratio analysis of <sup>18</sup>F-fluorodopa uptake in striatal subregions separates patients with early parkinson disease from healthy controls. *J Nucl Med* 2009; 50: 893-899.
- [5] Logan J, Fowler JS, Volkow ND, Wang GJ, Ding YS and Alexoff DL. Distribution volume ratios without blood sampling from graphical analysis of PET data. *J Cereb Blood Flow Metab* 1996; 16: 834-840.

## Quantification in $^{18}\text{F}$ -FDOPA PET

- [6] García-Gómez FJ, García-Solís D, Luis-Simón FJ, Marín-Oyaga VA, Carrillo F, Mir P and Vázquez-Albertino RJ. Elaboration of the SPM template for the standardization of SPECT images with  $^{123}\text{I}$ -loflupane. *Rev Esp Med Nucl Imagen Mol* 2013; 32: 350-6.
- [7] Abedelahi A, Hasanzadeh H, Hadizadeh H and Joghataie MT. Morphometric and volumetric study of caudate and putamen nuclei in normal individuals by MRI: effect of normal aging, gender and hemispheric differences. *Pol J Radiol* 2013; 78: 7-14.
- [8] Mai J, Assheuer J and Paxinos G. Atlas of the human brain. San Diego: Academic Press; 1997.
- [9] Lidstone SC, Schulzer M, Dinelle K, Mak E, Sossi V, Ruth TJ, de la Fuente-Fernández R, Phillips AG and Stoessl AJ. Effects of expectation on placebo-induced dopamine release in Parkinson disease. *Arch Gen Psychiatry* 2010; 67: 857-865.
- [10] Klein A and Tourville J. 101 labeled brain images and a consistent human cortical labeling protocol. *Front Neurosci* 2012; 6: 171.
- [11] Struck AF, Hall LT, Kusmirek JE, Gallagher CL, Floberg JM, Jaskowiak CJ and Perlman SB.  $^{18}\text{F}$ -DOPA PET with and without MRI fusion, a receiver operator characteristics comparison. *Am J Nucl Med Mol Imaging* 2012; 2: 475-482.